La mer 38 : 11–25, 2000
Société franco-japonaise d'océanographie, Tokyo

# Research on providing habitable environment for bivalves by use of artificial reefs

Hirokazu SUMI* and Akira WADA**

**Abstract** : In hope of developing technologies for providing habitable environment for bivalves (lamellibranchiata) by utilizing the wave attenuation function of artificial reefs, there is necessity of controlling sea waves and nearshore currents appropriately for the creation of such a favorable environment for shells. In this research, the effect of controlling the wave and nearshore current fields by artificial reefs was studied by hydraulic model tests and numerical calcuations.

In the hydraulic model tests, studies were made on how changes in the distance between dikes (opening width) and the length of dikes would affect flow patterns when installing several artificial reefs on the shore. These flow patterns were classified using the ratio of dike length to openig width. Based on this flow pattern classification, a steady circulation current was formed in nearshore current to allow inner water masses to catch larvae, making it consequently possible to prevent the dissipation of larvae.

In the numerical calculations, the wave and nearshore current fields were simulated with respect to Hamanaka Bay in Hokkaido, where five artificial reefs were installed with the aim of stabilizing the habitat of shells. In the hinterland of the artificial reef, wave heights were found about 30% less than those without artificial reef. Flow velocities wave weaker than those without artificial reef, thus making it possible to prolong the retention time of larvae and promote their implantation. Flow velocities at each calculation points were lower than the critical migration velocities of shells, enabling the artificial reef to prevent shells from being washed up and proving the effectiveness of such mounds in stabilizing the habitat.

**Key words** : *artificial reef, bivalve, hydraulic model test, numerical calculation*

## 1. Introduction

As one of measures to promote the harmonius coexistence of coastal-zone development and environmental conservation, the construction of coastal structures leading to the increased propagation of biological resources is sought for, and at the same time expectations are placed on the development of technologies to provide bivalves with an ideal habitable environment by utilizing the wave attenuation or sedimentation function of submerged mounds or artificial reefs (submerged breakwaters with wide crown).

In addition to the conventional coastal protection, the functions desired of these technologies include (1) promoting the implantation (agglomeration function) of bivalves' planktonic larvae and (2) securing a tranquil sea area and sandy-silt zone where postimplantation bivalves can live (habitat protection function). The artificial reef causes wave breaking on the crest and makes waves in the hinterland of the dike tranquil, so that the orbital velocity in the vicinity of the sea bottom due to a wave motion can be reduced and the overturn or exposure of shells can be prevented. Moreover, as the nearshore current is controllable, the diffusion prevention of planktonic larvae due to the current and the promotion of their implantation to sediments can be expected. It will be advantageous if the installation of such a artificial reef can

* Department of Civil Engineering, Nagoya University, Chikusa-ku, Nagoya, 464–8603
** College of Industrial Technology, Nihon University, Izumi, 1–2–1, Narashino, Chiba, 275–8575

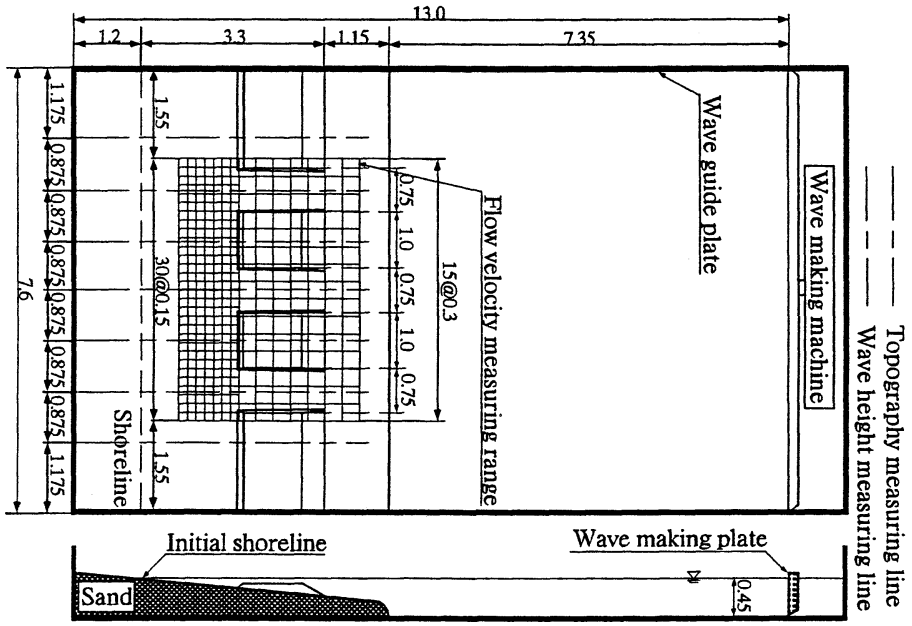


Fig. 1 Ourline of horizontal water tank(unit : m)

consequently stabilize the habitat suitable for the growth of bivalves.

In this research, therefore, taking into consideration that the creation of a favorable habitat for bivalves requires appropriate control of sea waves, nearshore current and littoral drift, which are the principal elements dominating the habitat environment, studies are made on the hydraulic characteristics that can be controlled by installing the artificial reef on the coast, from both aspects of hydraulic test and numerical simulation. Firstly, a movable bed test is conducted to obtain basic information on what kind of effect the changes in the length of a dike and the length of an opening will have on the flow pattern of a nearshore current or the formation of a circulation current and the stabilization of a shore when several artificial reefs are installed on the coast. Next, a numerical simulation is carried out with respect to Hamanaka Bay in Hokkaido where five submerged mounds are installed on the sandy beach, in order to study the effect of control in a wave field and nearshore current field by a group of submerged mounds.

## 2. Plane movable bed test on flow and littoral drift around the artificial reef

When installing several artificial reefs on the coast, a general practice is to install an opening between dike bodies. At this time, changing the dike length of the artificial reef and the length of the opening generates a characteristic nearshore current owing to changes in the height of transmitted waves which pass through above the dike and the opening, thereby causing the coastal topography to change, as is known by various kinds of past research (for example, UDA and KOMATA, 1987). However, it is hard to say that sufficient explanations have been made on hydraulic characteristics concerning the relation between flow patterns and shore changes when the dike length and opening width are changed. In this chapter, therefore, studies are carried out to determine what kind of effect the dike length and opening width will have on the flow pattern, the formation of a circulation current and the stability of a shore when several artificial reefs are installed.

### 2.1. Test method

The test was conducted using a horizontal

Table 1. Test cases and flow patterns

| Case No. | Dike length Lr(m) | Opening width W (m) | Offshore distance Y (m) | Flow pattern | Illustration |
|---|---|---|---|---|---|
| 1 | 2.0 | 0.3 | 1.8 | On-offshore current | Fig.3 (a) |
| 2 | 2.0 | 0.8 | 1.8 | Stable circulation current | |
| 3 | 1.0 | 0.22 | 1.8 | Unstable circulation current | Fig.3 (b) |
| 4 | 1.0 | 0.8 | 1.8 | Stable circulation current | Fig.3 (c) |
| 5 | 1.0 | 1.3 | 1.8 | Stable circulation current | |

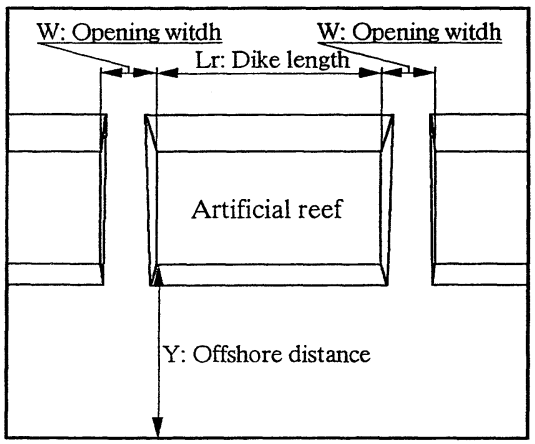


Fig. 2 Plane parameters of artificial reef.

wave-making tank (measuring 13.0 m long, 7.6 m deep and 0.5 m high) (see Fig. 1). Froude similitude was used as a law of similarity. The scale of a non-distorted model is 1/50, and the shore model is an artificial reef model installed as a rubble mound using silica sand of $d_m$=0.19 mm in median grain size with crushed stone weighing 3 to 4 g placed on the initial gradient of i=1/15. The dike has the following section parameters : s=1/3 in inclination of slope, B=1.0 m in crown width, d=14.0 cm in body height, R=6.0 m in submerged depth of crown. Plane parameters consist of dike length Lr, opening width W and offshore distance Y as shown in Fig. 2, and these were combined as shown in Table 1. As working wave conditions, $H_I$=6.0 m in incident wave height, T=1.13 s in period and 0° in wave direction (perpendicular to the shoreline) were applied for 5 hours.

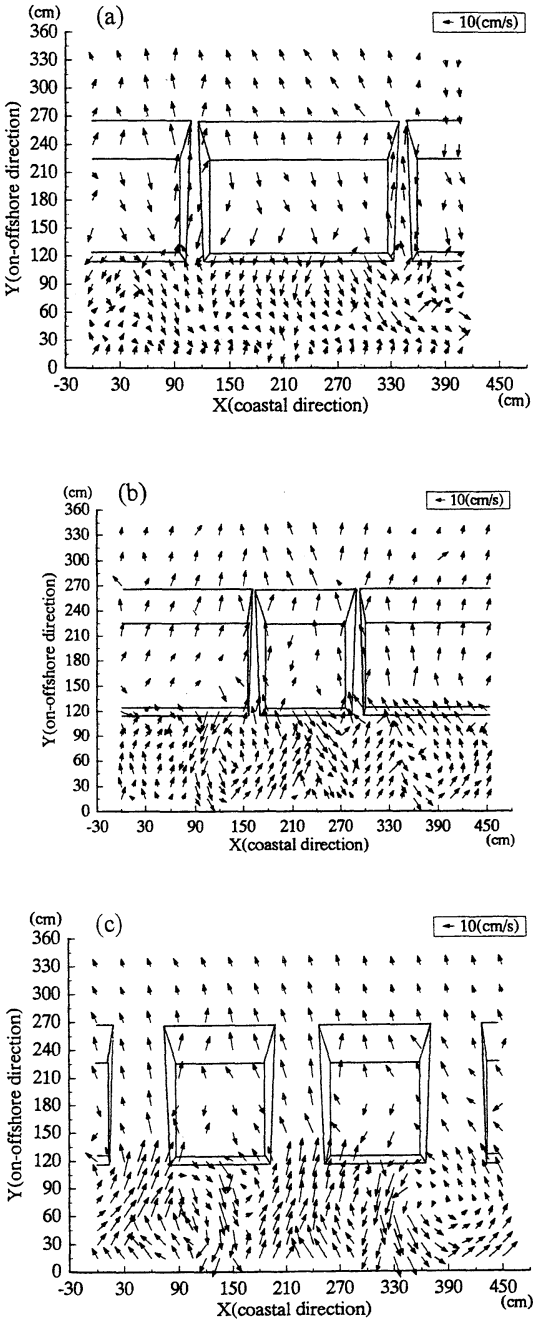


Fig. 3 Nearshore current aronund the artificial reef, (a) dike length : 2.0m, opening widht: 0.3 m, Case 1, (d) dike length: 1.0m, openingwidht: 0.22m, Case 3 and (c) dike length: 1.0m, openig width: 0.75m, Case 4.

The flow pattern of a nearshore current, the topography of a shore and the distribution of wave heights were measured. To determine the flow pattern of the nearshore current, as shown in Fig. 1, the velocity of flow was measured using an electromagnetic current meter at about 350 points around the artificial reef in the square grid divided at intervals of 30 cm from the offshore side to the toe of slope and at intervals of 15 cm at the back of the dike. At the same time, observations were made of flow patterns by means of floats and recorded with an 8 mm video camera from top of the water tank. The topography of the shore and the distribution of wave heights were measured at intervals of 20 cm in the on-offshore direction by installing a measuring line in the direction perpendicular to the shoreline against the combination of each test plane.

### 2.2. Test results and considerations

2.2.1. Nearshore current around the artificial reef

To carry out studies on the nearshore current around the artificial reef, an attempt here is made to identify the correlation between each test case concerning flow patterns which vary according to the setting of dike length and opening width, Figures 3(a), (b) and (c) indicate respectively the velocity distributions of (1) on-offshore current (Case 1), (2) unstable circulation current (Case 3) and (3) stable circulation current in the hinterland of the dike (Case 4).

In Cases 1 and 2 where the opening width was changes as W=0.3 m and 0.75 m with the same dike length (Lr=2.0 m), the current was flowing in the offshore direction in both the offshore side of the dike and the opening. In the hinterland, in Case 1 with a narrow opening width, the current flowing in the on-offshore direction was recognized, while in Case 2 with a large opening width two circulation currents were found generated. In Cases 3, 4 and 5 where the opening width was changed as W=0.22 m, 0.75 m and 1.25 m with the same dike length (Lr=1.0 m), the current flowing in the offshore direction was generated in the offshore side of the dike and the opening. In the hinterland, in Case 3 with a narrow opening, the onshore current and rip current were irregularly recognized and an indistinct circulation current was found generated, while in Case 4 whose opening width is between Case 3 and Case 5, one circulation current was found formed at the back of the dike. Also, in Case 5 with the largest opening width, two circulation currents were found generated.

Thus, it is evident that if the dike length is constant, the larger the opening width is the more likely the circulation current is generated. It is also evident that in the offshore side of the dike and the opening, the flow pattern is in the offshore direction irrespective of dike length and opening width, while in the onshore side of the dike the flow pattern of a nearshore current varies with the setting of dike length and opening width. In addition, to promote the implantation of planktonic larvae and the reduction of diffusion through the use of the artificial reef, the generation of a stable circulation current in the habitat is desired and at the same time, it is necessary to establish a criterion for setting the dike length and opening width.

Figure 4 shows the relation between Lr/W and Lr/Y, in comparison with the past research results. The marks (○,⌀,▽,□) indicate the test results obtained by UDA *et al.* (1987), while those shown in black are the test results obtained in this research. The case in which the circulation current is generated and the case in which the on-offshore current is predominant indicate results almost similar to the past research, and it can be considered that the flow pattern around the artificial reef is governed by Lr and W. Accordingly, from the test results obtained in this research and the research results obtained by UDA *et al.* (1987), it can be assumed that the flow-pattern in the hinterland of the dike consists of three conditions, i. e., $0 < Lr/W \leq 4$ as a domain in which a stable circulation current is generated, $4 < Lr/W \leq 6$ as a domain in which an unstable circulation current is generated, and $6 < Lr/W$ as a domain in which no circulation curent is generated. Using this flow-pattern, a steady circulation current is allowed to be formed in the nearshore current, with planktonic larvae trapped in its inner water mass so that the dissipation of

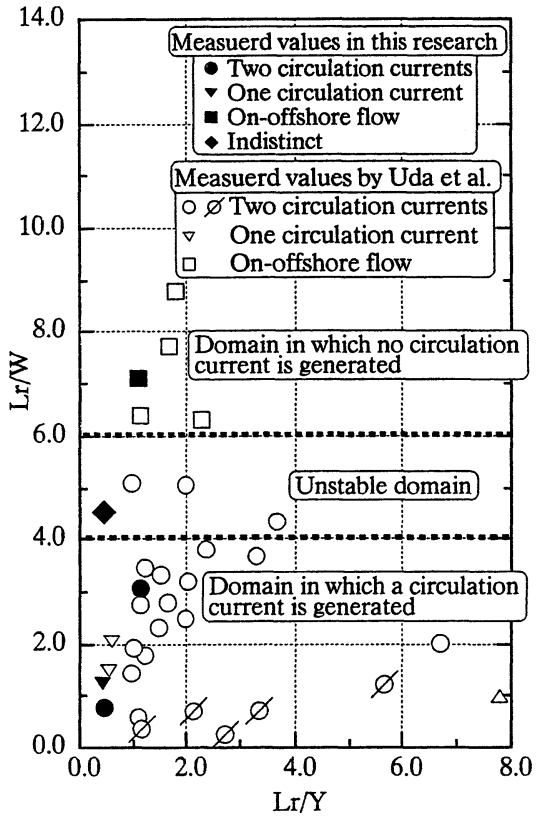


Fig. 4 Flow pattern occurrence classification.

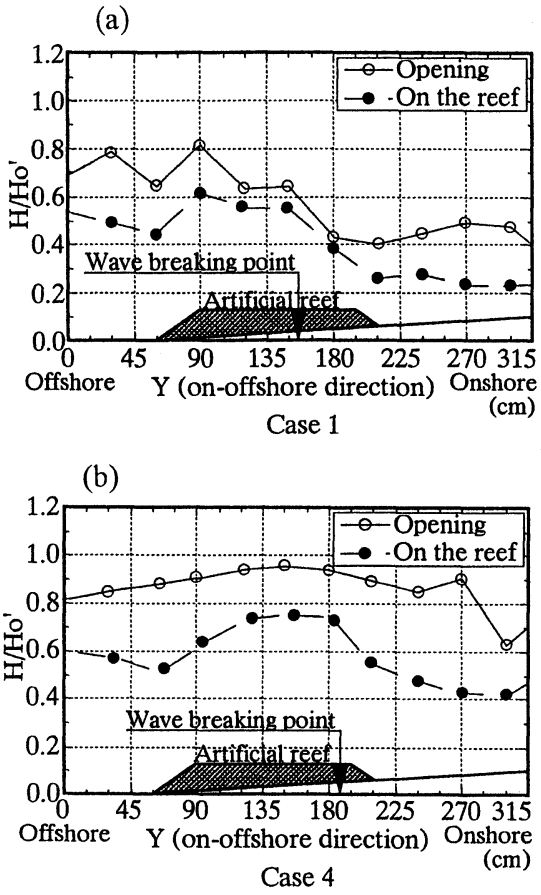


Fig. 5 Wave height distribution in the on-offshore direction of artificial reef, (a) dike length: 2.0m, opening width: 0.3m and (b) dike length: 1.0m, opening width: 0.75m.

larvae can be prevented.

2.2.2. Wave height distribution

Figure 5 shows the comparison of changes in wave height between the case where the on-offshore current is generated and the case where the circulation current is generated. The longitudinal axis in the figure indicates the plot of H/Ho′ in the on-offshore direction. H is wave height obtained from the test, Ho' is wave heigth due to offshore diffraction or refraction. Figure 5(a) shows changes in wave height in the case where no circulation current is generated, while Figure 5(b) shows those in the case where one circulation current is generated in the hinterland. The wave height on the reef in the hinterland of the dike is showing an attenuation of about 50% in Fig. 5(a) and about 40% in Fig. 5(b). On the other hand, the wave height in the opening is attenuating in Fig. 5(a), while in Fig. 5(b) the incident wave reaches the onshore side without undergoing attenuation and the wave-height difference on the reef and in the opening is increasing as compared with Fig. 5(a). Thus, assuming that the difference of wave height on the reef and in the opening is related to the generation of the circulation current, Fugure 6 shows the relation between W/Lr and nondimensional wave-height difference (Hm-Ht)/Ho′ obtained by making the difference between wave height Hm in the opening and transmitted wave height Ht in the hinterland dimensionless by Ho′. From this fugure, it is evident that the larger W/Lr and the smaller Lr/Y the larger

becomes the difference in wave height on the dike and in the opening and the more likely the circulation current is generated.

2.2.3. Topographic change

It can be considered that the phenomenon of littoral drift around the artificial reef is related to a nearshore current. To grasp the migration of sand caused by the nearshore current, therefore, the horizontal distribution of coastal topographic changes from the initial slope were obtained from the coastal topography 5 hours after starting wave generation, as shown in Figs.7 and 8. Although similarity laws were not sufficiently established in the test on littoral drift, topographic changes around structures due to currents were studied qualitatively and the Froude similitude was followed because of placing emphasis on the fluid motion.

Figure 7 shows topographic changes without artificial reef. From the neighborhood of the shoreline up to Y=125 mm, sand erosion takes place and a trough is generated. Up to Y=150 to 250cm, bar-type seabed topography with sand deposition and growth of a longshore bar is recognized.

Figure 8(a) shows topographic changes in Case 1 where a current in the on-offshore direction is generated. In the hinterland, an on-offshore sediment movement occurs due to the onshore current and rip current generated at the back of the dike, causing erosion from the shoreline up to Y=100 cm. The sand deposition is found on the foreshore. Fugure 8(b) shows topographic changes in Case 3 where an unstable current is generated. Up to X=0 to 50 cm, sand deposition is recognized from the back of the dike to the shoreline, while sand erosion is recognized up to X=500 to 350 cm. It can be considered that this complicated beach configuration is related to the generation of an irregular onshore current and rip current at the back of the dike. Also, eroded sand is deposited near the toe of slope and on the foreshore. Figure 8(c) shows topographic changes in Case 4 where a stable circulation current is generated. Sedimentation is recognized near the toe of slope and on the foreshore, and erosion is found from Y=80 cm to the shoreline. Considering the balance of sand, it seems that

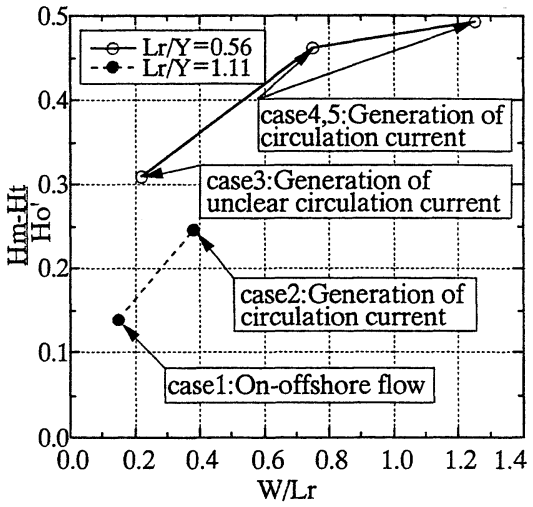


Fig. 6 Relation between wave height difference and generation of circulation current.

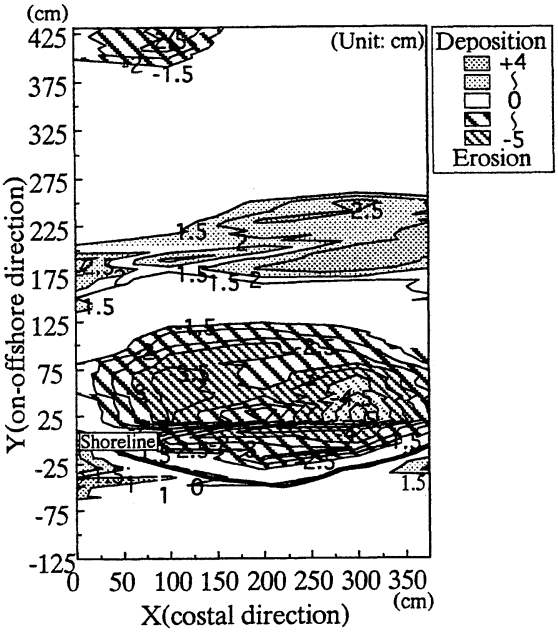


Fig. 7 Topographical changes without artificial reef.

sedimentation near the toe of slope was transported owing to the circulation current, indicating that the dike prevented the runoff of sand to the offing. The shoreline was advancing about 40 cm greater than that without artificial reef, the growth of steps was recognized and

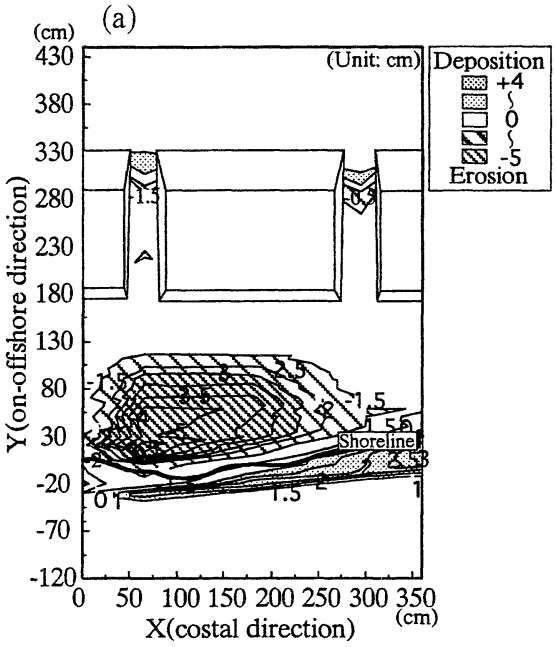


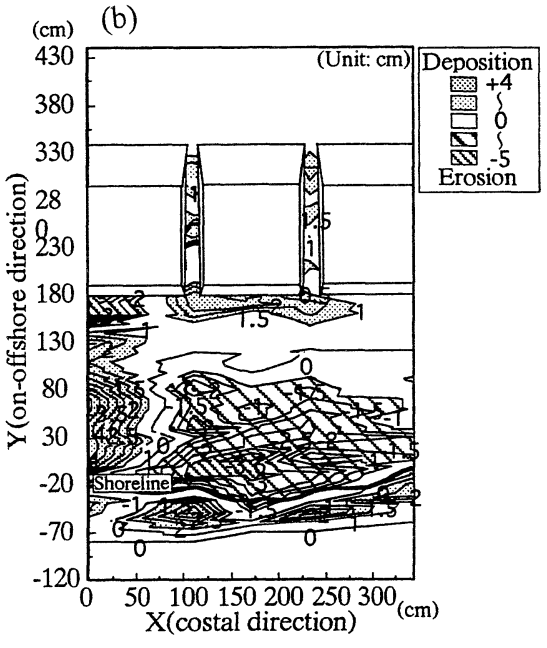


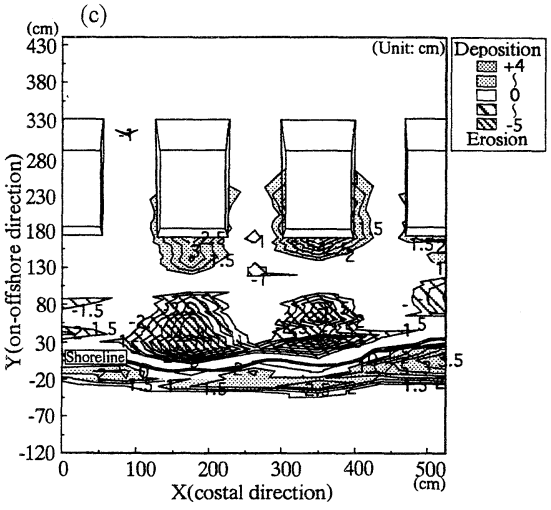


Fig. 8 Topographical changes around the artificial reef, (a) dike length: 2.0m, opening width: 0.3m, Case 1, (b) dike length: 1.0m, opening width: 0.22m, Case 3 and (c) dike length: 1.0m, oprning width: 0.75m, Case 4.

the foreshore was found extended, thus conspicuously indicating the effect of littoral drift control by the artificial reef.

The stabilization of sediments becomes an important problem when we try to reduce wear due to the overturn and exposure of bivalves. Topographic changes in the case where artificial reefs are installed on the beach vary with the flow pattern of a nearshore current. In the case where the on-offshore flow is predominant, sand deposition takes place on the foreshore only. In the case where a circulation current is generated, sand deposition takes place near the toe of slope and on the foreshore. Also, the shoreline advances greater than that without artificial reef, and the inshore erosion zone becomes smaller. Thus, the artificial reef minimizes topographic changes in the hinterland and promotes the stabilization of sediments, thereby possibly contributing to reducing the on-the-sand exposure and swash of shellfish larvae and adult shells.

### 3. Numerical simulations on wave field and nearshore-current field

In Hamanaka Bay which is located in the eastern part of Hokkaido as shown in Fig. 9, five artificial reefs are installed along the sand coast for the purpose of stabilizing the habitat of bivalves. The mouth of Hamanaka Bay is opening eastward and has a width of about 6

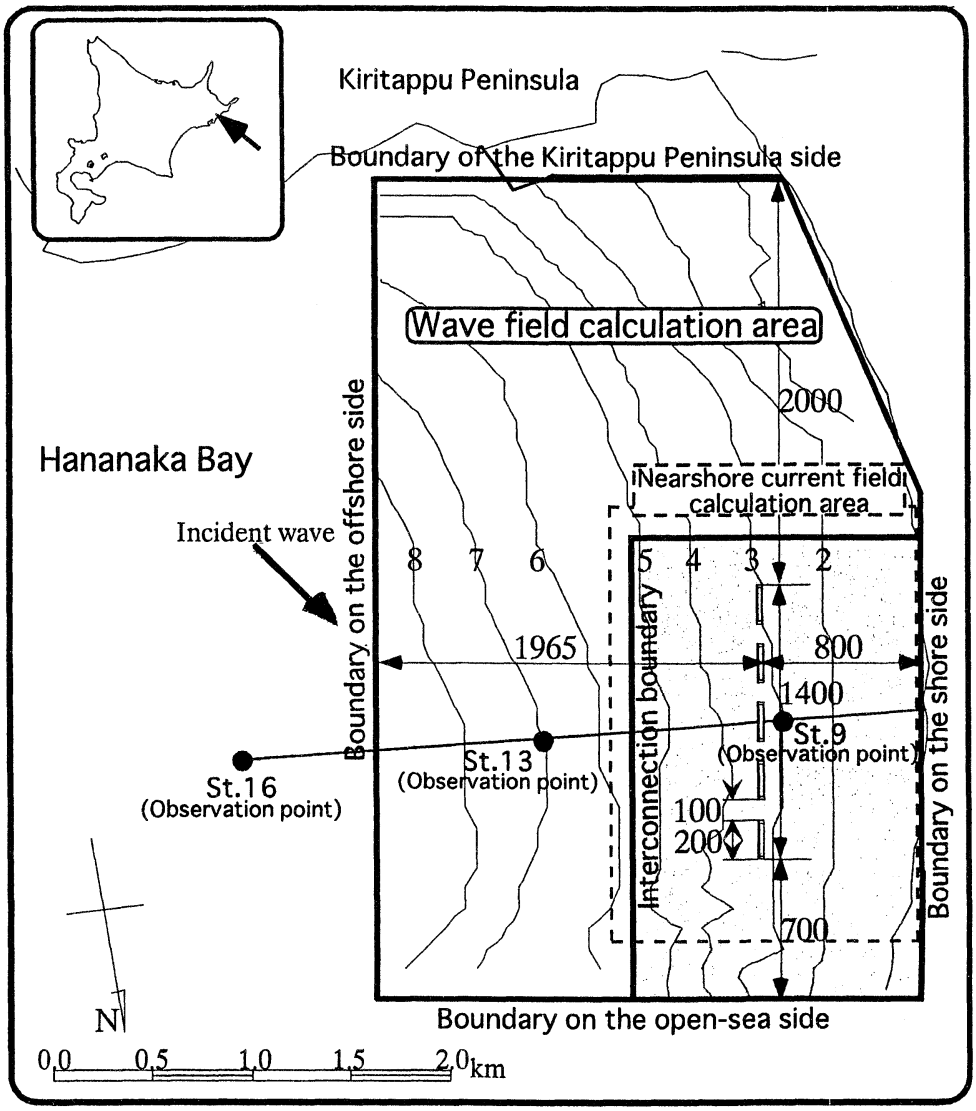


Fig. 9 Study area(unit: m).

km. The depth of water in the bay is less than 20 m, with a gentle gradient (1/280). According to Mimura et al. (1996), bivalves are the major fishery resources in this bay, though the number of bivalves living in the bay is on the decrease and there is concern about the upkeep of these resources.

To develop technologies relating to the creation of bivalve fish grounds, it is pointed out that sea waves and nearshore currents are important elements in the formation of a habitat (ITOSU, 1985). In the field survey carried out in the summer of 1996, however, wave and current observations were conducted only at three points in the bay, which was insufficient to grasp in detail the condition of waves and flows in the vicinity of artificial reefs. In this report, therefore, a description is made on the numerical simulations which are conducted on the wave field and nearshore current field around the artificial reefs, and comparisons are made with on-site observed values, to examine

the effect of controlling the sea waves and nearshore current by a group of artificial reefs.

### 3.1. Numerical simulation on the wave field

The calculation of a plane wave field may be broadly classified into two methods, depending on how waves are dealt with. That is to say, one method deals with waves as the equation of energy and another method deals with waves as the equation of motion (HONMA and HORIKAWA, 1985). A typical wave model of the former is the energy balance equation (hereinafter called EBE), while that of the latter is the time-dependent mild slope equation (TDMSE). EBE is a wave model which can simultaneously solve the refraction of multidirection random waves and the wave shoaling. Howaver, the field of progressive waves whose single direction can be defined at each calculation point is a precondition for this model, thereby making it difficult to apply the model to the analysis of a field in which waves are superimposed owing to reflection or diffraction. TDMSE is a model that can comprehensively evaluate the principal deformations of waves in the shallow sea, i. e., shoaling, refraction, diffraction, reflection and breaking, though its handling is limited to regular waves.

The wave models have their own characteristics, and it is therefore necessary to determine the scope of application appropriately according to purposes. For example, in the case that (1) offshore waves suffer only refraction or shoaling owing to the effect of seabottom topography or (2) waves suffer attenuation in height simultaneously owing to diffraction, reflection or breaking caused by the effect of coastal structures built near the shoreline in the shallow sea, it is necessary to use a wave model which can appropriately evaluate the deformation of waves in the respective sea areas.

Then, to estimate the plane wave field around the artificial reefs built in the coastal area of Hamanaka Bay, interconnection calculations are carried out on the two wave models, EBE and TDMSE. That is to say, in the offing where waves are not affected by structures, EBE is used, while in the sea area where waves are affected by structures, TDMSE is used to estimate the wave field in the sea area concerned.

### 3.2. Basic equations

EBE, to which the wave-breaking attenuation term is added, is given by equation (1).

$$\frac{\partial}{\partial x}(SC_g\cos\theta)+\frac{\partial}{\partial y}(SC_g\sin\theta)+\frac{\partial}{\partial\theta}\left\{S\frac{C_g}{C}\left(\sin\theta\frac{\partial C}{\partial x}-\cos\theta\frac{\partial C}{\partial x}\right)\right\}=-\varepsilon_b' S \tag{1}$$

Where, $S$ : Direction spectrum, $C_g$ : Group velocity, $C$ : Wave velocity, $\theta$ : Wave direction, $\varepsilon_b$ : Wave-breaking attenuation term.
Also, TDMSE, to which the wave-breaking attenuation term is added, is given by equations (2a, 2b) and equation (3).

$$\frac{\partial Q_x}{\partial x}+C^2\frac{\partial\zeta}{\partial x}+f_D Q_x=0 \tag{2a}$$

$$\frac{\partial Q_y}{\partial y}+C^2\frac{\partial\zeta}{\partial y}+f_D Q_y=0 \tag{2b}$$

$$\frac{\partial\zeta}{\partial t}+\frac{1}{n}\left(\frac{\partial nQ_x}{\partial x}+\frac{\partial nQ_y}{\partial y}\right)=0 \tag{3}$$

Where, $Q_x$, $Q_y$ : Line flow rate, $\zeta$ : Water-surface fluctuation, n : Ratio of wave velocity to group velocity, $f_D$ : Wave-breaking attenuation.

The actual numerical calculations are carried out by converting these basic equations into finite-defference equations against the array of calculation points for various parameters on the grid mesh and giving boundary conditions as necessary.

### 3.3. Wave-field calculation results

At first, in order to examine the effect of artificial reefs on the wave field, the distribution of wave heights in Hamanaka Bay was calculated by applying TDMSE to the seabottom topography before and after installing the artificial reefs in the wave-field calculation area (with and without hatch) shown in Fig. 9. In this calculation area, it is necessary to pay attention to the range of effects the artificial reefs or coastal topography have on sea waves, so conditions were established in such a way that the diffraction effect of waves from Kiritappu

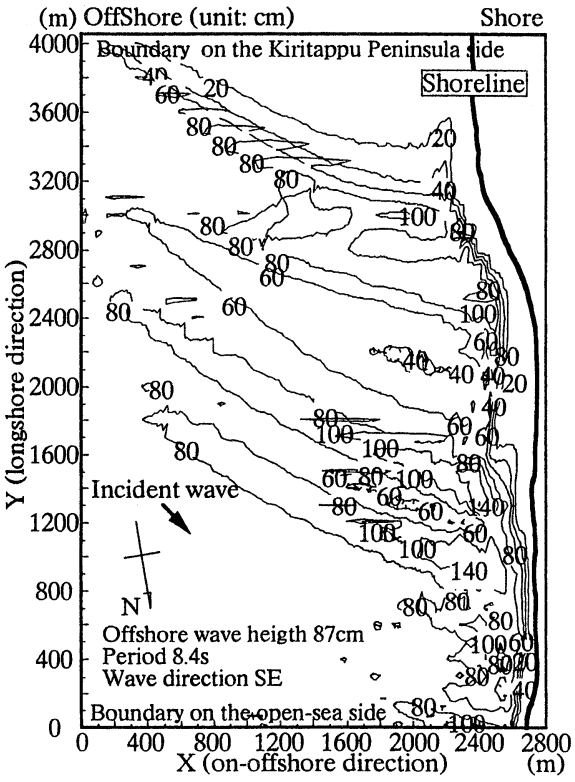


Fig. 10 Results of wave field calculations before installing artificial reefs (TDMSE).

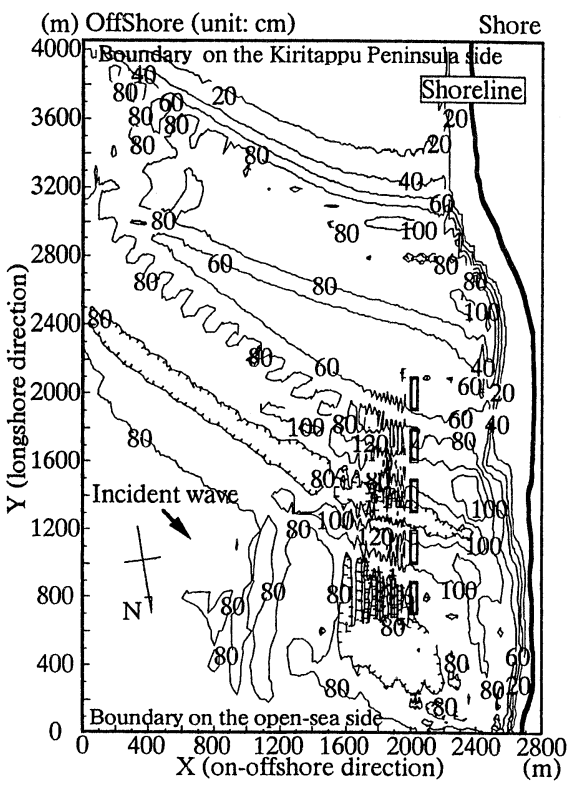


Fig. 11 Results of wave field calculations after installing artificial reefs(TDMSE).

Peninsula could be considered, including all groups of 5 artificial reefs. The boundary condition was established as an incident boundary which gives a significant wave parameter in the offshore boundary. The boundary on the side of Kiritappu Peninsula was assumed to be a closed boundary without input of line flow rate. The boundary on the open-sea side and the boundary on the shore side were assumed to be open boundaries. Each artificial reef has the following parameters : 200 m in dike length (Lr), 100m in opening width (W) and 800m in offshore distance (Y), which are similar to those on the site. Working wave conditions are as follows : offshore wave height Ho=87cm, period T=8.4 s and wave direction SE, according to typical wave parameters from on-site observations.

Under these conditions, calculations were made on the plane wave field by applying TDMSE to the seabottom topography before and after installing the artificial reefs, and their results are shown in Figs. 10 and 11, respectively. Looking at the wave field before installing the artificial reefs, the waves entering from the direction of SE are affected by diffraction from Kiritappu Peninsula which is located in the south of the bay, and the wave height is small in the vicinity of the peninsula. The wave height in the on-offshore direction in the area near Y=1500m underwent a change in refraction due to offshore seabottom topography, thereby causing shoaling toward the coast. After growing into about 140cm, the wave height faces the breaking point, attenuates and reaches the shoreline. Looking at the wave field after installing the artificial reefs, reflected waves are produces in the front part of the breakwater, while in the hinterland the wave height is attenuating about 30% as compared with that before installing the artificial reefs. Thus, the wave control effect of artificial reefs

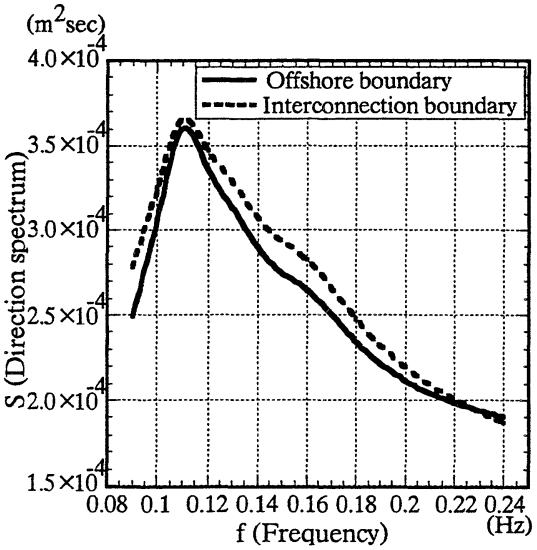


Fig. 12 Main wave direction spectrum.

is evidently seen, possibly providings a favorable place for bivalves to live in.

Next, the sea area (with hatch) around the artificial reefs shown in Fig. 9 was considered as a study area, and interconnection calculations were carried out to estimate the wave field by applying EBE in the sea off the study area and using TDMSE in the sea within the study area. When interconnecting the two wave models, significant wave parameters were obtained from the results of EBE direction spectrum calculations as input conditions to TDMSE.

The boundary condition in the EBE calculation area (without hatch + with hatch) was established as the incident boundary which gives a direction spectrum so that the irregularity of waves can be considered by on-site observations. The open-sea boundary and coastal boundary are assumed to be open boundaries, with the same spectrum in and outside the calculation area. The boundary on the side of Kiritappu Peninsula is assumed to be a closed boundary, with no energy input.

The results of direction spectrum calculations by EBE under the conditions mentioned above are as follows. Figure 12 shows the main wave direction spectrum between the offshore boundary and the interconnection boundary,

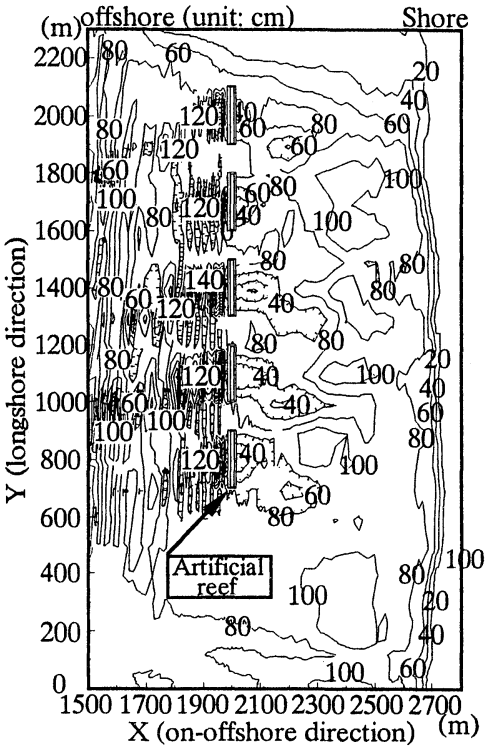


Fig. 13 Results of interconnection calculations of the wave field.

with the energy of waves concentrated in the neighborhood of f=0.11 Hz. The total energy of waves is obtained from the direction spectrum, which is the converted into significant wave height $H_{1/3}$. Consequently, $H_{1/3}$ is about 78 cm. The distribution of wave heights in the interconnection calculation with this significant wave height given to TDMSE as input condition in the interconnection boundary, is shown in Fig. 13. The distribution shows that in the front part of the artificial reefs, reflected waves are produced ; in the hinterland, the wave height attenuates and after that, waves are reproduced causing the wave height to increase again. Comparing the wave height distributions shown in Figs.13 and 11, the tendency of the wave height to reach about 100cm in the coastal direction over X=2400～2500m is appearing in both, though difference is recognized in the distribution of wave heights in the coastal direction near X=2100m. This is due to

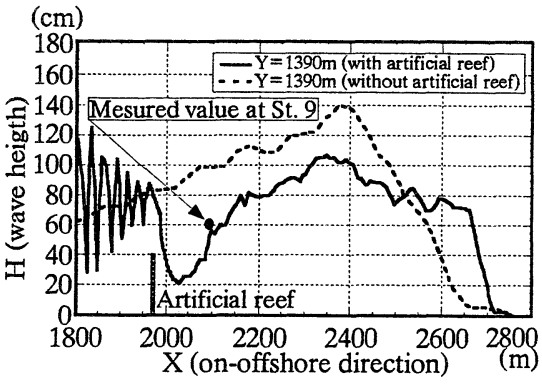


Fig. 14 Comparison of calculated values and on-site observed values.

the effect of difference in the wave height distribution in the neighborhood of the interconnection boundary. That is to say, in Fig. 11, a sign wave is given in the offshore boundary, and a solution by TDMSE is calculated, hence the wave-height fluctuation in the entire calculation area becomes conspicuous due to the phase interaction of waves. On the other hand, EBE solves the energy transport status of irregular waves, thereby obtaining a solution to more smoothened wave-height distribution than TDMSE. In Fig. 13, this smoothened wave-height distribution is input in the interconnection boundary, possibly causing a difference from Fig. 11. In Fig. 14, changes in wave height with and without artificial reefs at Y=1390m shown in Figs.10 an 13 are plotted in the on-offshore direction to make comparison with the on-site observed values. The wave height with artificial reefs in the hinterland is smaller than that without artificial reefs, and in the neighborhood of X=2000m, the wave height is showing a sudden decrease owing to forced breaking by the artificial reefs. It seems that such a decline in the wave height reduces the bottom orbital velocity which is in proportion to the wave height, making it possible to contribute to the increased stability of the habitat. Also, the calculated values are almost similar to the observed values at St. 9.

When the identification of a wave phenomenon that can be controlled by coastal structures for the habitat stabilization of bivalves becomes an important problem, as in Hamanaka Bay, it will be more effective to apply TDMSE which can comprehensively evaluate all wave deformations around the artificial reefs and apply EBE in the sea area where waves waves are not affected by the artificial reefs. As one of the advantages to make such interconnection calculations, shorter computation time is pointed out, with the CPU occupation time for interconnection calculations being about 1/4 of TDMSE only.

### 3.4. Numerical simulation on the nearshore current field

When an attempt is made to control the dissipation of bivalves' planktonic larvae or promote their implantation, a possible method is to weaken the velocity of flow or change the flow patten by installing artificial reefs. In this section, therefore, numerical simulation is carried out on the nearshore current filed to examine the effect of the artificial reefs installed in Hamanaka Bay on the flows in the surrounding sea areas.

### 3.5. Basic equation

The flow near the coastal zone, which occurs due to sea waves, is generated owing to the gradients of radiation stresses in the on-offshore direction and coastal direction. The orthogonal coordinates are taken within the horizontal plane and defines the on-offshore axis in the x direction and the longsshore axis in the y direction. The equation of continuity is as described below with each component of the mean flow assumed to be U and V and the mean sea level, $\zeta$.

$$\frac{\partial \xi}{\partial t}+\frac{\partial U(h+\xi)}{\partial x}+V\frac{\partial V(h+\xi)}{\partial y}=0 \tag{5}$$

Also, the equation of motion containing the radiation stress is given by the following :

$$\frac{\partial U(h+\xi)}{\partial t}+U\frac{\partial U(h+\xi)}{\partial x}+V\frac{\partial V(h+\xi)}{\partial y}$$
$$=-g(h+\xi)\frac{\partial \xi}{\partial x}$$
$$+\frac{\partial}{\partial x}\left\{\varepsilon_x\frac{\partial U(h+\xi)}{\partial x}\right\}+\frac{\partial}{\partial y}\left\{\varepsilon_y\frac{\partial U(h+\xi)}{\partial y}\right\}$$
$$-\frac{1}{\rho}\frac{\partial S_{xx}}{\partial x}-\frac{1}{\rho}\frac{\partial S_{xy}}{\partial y}-\tau_{bx} \tag{6a}$$

$$\frac{\partial U(h+\xi)}{\partial t}+U\frac{\partial U(h+\xi)}{\partial x}+V\frac{\partial V(h+\xi)}{\partial y}$$
$$=g(h+\xi)\frac{\partial \xi}{\partial y}$$
$$+\frac{\partial}{\partial x}\left\{\varepsilon_x\frac{\partial V(h+\xi)}{\partial x}\right\}+\frac{\partial}{\partial y}\left\{\varepsilon_y\frac{\partial V(h+\xi)}{\partial y}\right\}$$
$$-\frac{1}{\rho}\frac{\partial S_{yx}}{\partial x}-\frac{1}{\rho}\frac{\partial S_{yy}}{\partial y}-\tau_{by} \qquad (6b)$$

Where, the fourth and fifth terms in the right side are radiation stress terms which are difined as the excess momentum flux of waves, while the sixth in the right side is a seabottom friction term.

Eddy viscosity coefficients $\varepsilon_x$ and $\varepsilon_y$ are expressed by the equation (7) according to the hypothesis of LONGUET-HIGGINS (1970).

$$\varepsilon_{x,y}=N\ell\sqrt{g(h+\xi)} \qquad (7)$$

Where, N : Non-dimensional constant in the order of 0.01, $\ell$ : Offshore distance Numerical calculations are perfomed by converting equation (5) and equations (6a, 6b) into the finite difference equation against calculation points for various parameters defined on the grid mesh. Meanwhile, the radiation stress of progressive waves which become a nearshore-current driving force was calculated using the wave energy and wave direction from the results of wave-field calculations and was given to the equation of motion.

### 3.6. Results of nearshore-current field calculations

The nearshore-current study area was established by paying attention to that the range of effects by a group of artificial reefs should be included as shown in Fig. 9, the depth contour changes gently in the longshore direction, etc.

Figure 15 shows the results of calculations on the nearshore current field before installing the artificial reefs. The circulation flow centering around X=2400m, Y=1250m and X=2500m and Y=1500m is recognized. These positions correspond to a portion in which the wave height declines from maximum 140cm to about 60~80cm in the longshore direction, according to the results of wave-field calculations shown in Fig. 10. If the wave-height distribution is not uniform in the longshore direction, the sea-

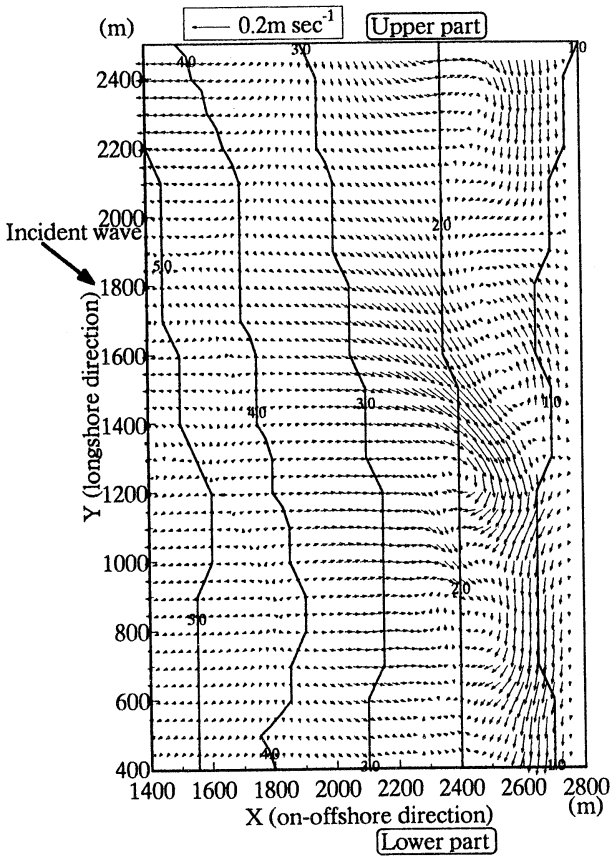


Fig. 15 Results of calculations on the nearshore current before installing artificial reef.

water accumulated near the shore under equilibrium condition must be returned to the offing, thereby generating such an offshore current (trip current). As a current that compensates the rip current, the longshore current develops in the almost same direction as the incident angle of waves, producing a large velocity value. HARRIS (1969) assumes that the frequency of causing such an assymetric-cell nearshore current is about 50% of the nearshore current system in the case where waves enter obliquely in the natural coast.

Figure 16 shows the results of calculations on the nearshore current field after installing the artificial reefs. For radiation stress, the values obtained from the results of wave-field calculations shown in Fig. 13 were used. The

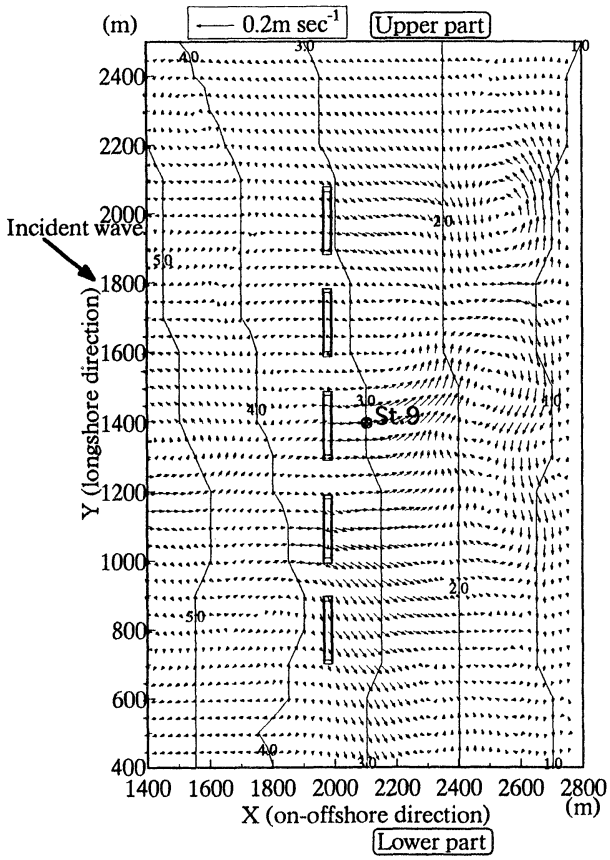


Fig. 16 Results of calculations on the nearshore current after installing artificial reef.

greater part of the flow near the shore is heading from the upper part toward the lower part, and the flow direction in the vicinity of X =2500m, Y=900m where the flow velocity becomes weak is changed toward the offshore side, forming a large circulation flow in the hinterland zone. Also, part of it heads from the lower part toward the upper part, which is contrary to the incident direction, and overlaps the current which flows downward from the upper part, forming a small counterclockwise circulation flow. If waves enter obliquely against a group of artificial reefs, a bilaterally assymetric circulation flow is generated in the hinterland zone, and its velocity is weakened near the shore as compared with the case where there is no artificial reef. The velocity obtained by onsite observations at St.9 was about 4 cm sec$^{-1}$ and the velosity at the calculation point corresponding to St.9 was 4.2 cm sec$^{-1}$, hence it can be said that the observed value agreed almost with the calculated value.

The nearshore current mainly affects the migration of shells, the diffusion of egge and larvae and the promotion of implantation. WATANABE (1982) reports that the critical velocities for migration of bivalves (specific gra vity : 1.32) whose shell lengths are 1, 3 and 5 cm are about 29, 40 and 50 cm sec$^{-1}$, respectively, in the case where there are sand ripples on the seabottom. In the nearshore-current calculation in the case where artificial reefs were installed, the maximum velocity is estimated at about 12.6 cm sec$^{-1}$, which is lower than the critical velocity for the migration of shells, and it can therefore be considered possible to prevent the runup of shells exposed from the bottom surface. Also, in the water area behind the mound, the velocity with artificial reefs was found weaker than that without artificial reefs, thus the retention time of larvae within the water area becomes longer, possibly promoting their implantation.

## 4. Conclusions

With the habitat stabilization of bivalves in mind, plane movable bed tests on the nearshore current and littoral drift phenomena around the artificial reef and numerical simulations on the wave field and nearshore current field around a group of artificial reefs installed in Hamanaka Bay were carried out, and hydraulic characteristics were examined. As a result, the following conclusions were drawn up :

(1) The peculiar nearshore current which is generated around the artificial reef depends on changes in the length of the dike and the length of the opening width, and the longer the opening width the more likely the circulation flows occurs. If the classification of circulation flow occurrence patterns is indicated according to the dike length and opening width, it may be broadly classified into the following three zon es : Zone in which a stable circulation flow is generated with $0 < Lr/W \leq 4$, zone in which an unstable circulation flow is generated with $4 < Lr/W \leq 6$, and zone in which an on-offshore flow is generated with $6 < Lr/W$. Using this

flow pattern classification, a steady circulation flow is formed in the nearshore current and planktonic larvae are trapped in the water mass in it, so that the dissipation of larvae can be controlled.

(2) The wave height in the case where a group of artificial reefs were installed in Hamanaka Bay was found about 30% lower than that without artificial reefs. The nearshore current field generated a stable circulation flow by installing the artificial reefs, and the velocity of flow near the shore was found weakened. It can be considered that the control of sea waves and flows using these artificial reefs will mitigate the outflow of bivalves' planktonic larvae and promote their implantation, possibly leading to the creation of an ideal habitat.

Although this research is confined to a study on the control of waves and flows by the artificial reef, it will provide useful information in the foundamental stage to identify the hydraulic characteristics these structures give to the habitat.

**Acknowledgement**

The authors would like to express thanks to the Marine Ecology Research Institute which supplied measurement data on wave heights and flow velocities in Hamanaka Bay during this research.

**Reference**

HARRIS, T. F. W. (1969) : Nearshore circulation, field observetions and experimental inverstigations of an underlying cause in wave tanks. Symposium on Coastal Eng., South Africa, pp. 1–13.

HASEGAWA, H. (1996) : Hydraulic study on offshore submerged mounds for construction of bivalve propagation grounds. Proceedings of Coastal Engineering, **43**, 1056–1060.

HONMA, H., and S. HORIKAWA (1985) : Marine Environmental Engineering. Tokyo University Press, pp. 217–248.

ITOSU, C., and M. MIKI (1985) : Wave circulation flow in the abalone fishing ground-study on the generation mechanism of circulation flow and its generation test. Fishery and Civil Engineering, **22**, 47–57.

LONGUET-HIGGINS, M. S. (1970) : Longshore currents generated by obiquely incident sea waves. 2. J. Geophy. Res., **75**, 4421–4426.

MIMURA, N., Y. KOIBUSHI, Y. NAKAMURA, J. KITA and R. ISONO (1996) : Total analysis on the habitat distribution of surf clams (Spisula sachalinesis) and the physical environment. Proceedings of Coastal Engineering, **43**, 1051–1055.

UDA, T., and A. KOMATA (1978) : Method for design of artificial reefs. Civil Engineering Technical Data, **26**, 26–31.

UDA, T., A. KOMATA, and H. YOKOHAMA (1978) : Nears hore current and topographical changes around the artificial reef. 37th Proceedings of Coastal Engineering, pp. 337–341.

WATANABE, E. (1982) : Experimental research on the decrement of surf clams due to sea waves. Civil Engineering Laboratory Monthly Report, No. 351, pp. 3–15.

*Recieved September 23, 1999*
*Accepted May 31, 2000*